JOURNAL OF MATERIALS SCIENCE 29 (1994) 5183–5187

R-curve measurement of silicon nitride ceramics using single-edge notched beam specimens

S. SAKAGUCHI, N. MURAYAMA, Y. KODAMA, F. WAKAI
Government Industrial Research Institute, Nagoya 1-1, Hirate-cho, Kita-ku, Nagoya 462, Japan

R-curve behaviour of three kinds of silicon nitride-based ceramics has been studied using the single-edge notched beam (SENB) technique. If the notch is deep enough, the specimen shows stable fracture during the bending test, even when the sample is a brittle material. The conditions required to obtain stable fracture in the bending test are clarified by the analysis. The crack length of the specimen was also calculated from the changing load during the fracture test. In this study, coarse-grained silicon nitride shows a large increase of the *R*-curve. On the other hand, silicon nitride with silicon carbide whiskers shows no *R*-curve increase. The rise of the *R*-curve should be related to the microstructure of the ceramics, and especially to the grain size of the specimen, because silicon carbide whiskers are not large compared to the silicon nitride grains, and silicon carbide can reduce the grain growth of silicon nitride during sintering.

1. Introduction

Engineering ceramics, such as silicon nitride or silicon carbide, are expected to find use as structural materials, because of their excellent properties against heat and corrosion. The largest problem in the application of engineering ceramics is their brittleness, which causes fracture to occur instantaneously from defects in the material. Many studies have been carried out in attempts to improve the fracture toughness of ceramics.

If a material shows an increase of fracture resistance during crack extension, it can lead to an improvement in the brittleness of the material. This is the concept based on the *R*-curve behaviour. For example, silicon carbide whisker addition in silicon nitride is a typical case where this effect is obtained [1–5]. In this case, it is necessary to obtain the relation between crack length and the stress intensity factor for the fracture of the material [6–8].

To obtain this relation, it is necessary to extend the crack stably during the test in order to measure the change of load during the fracture test. However, stable fracture cannot be observed in the regular fracture test on ceramic materials. Therefore, the geometry of the test piece should be considered in fracture testing of ceramics.

Fracture toughness measurement using a chevron-notched beam is one of the most common techniques used to obtain stable fracture in ceramic materials [9, 10]. Although this technique is good for extending the crack stably, it has a triangular-shaped ligament part on the bending specimen, so that the fracture surface at the initial stage is very small, and it is very difficult to obtain the crack length with sufficient accuracy, from measurement of the changing compliance.

On the other hand, fracture toughness measurement using the single-edge notched beam (SENB) technique is well known, but this technique has been rarely applied for stable fracture of ceramics [6, 8], because it has a straight notch, and so it is believed that the specimen will always break instantaneously for brittle material.

In the present work we analysed the specimen shape required to break the SENB specimen stably. Three kinds of silicon nitride-based ceramics were then examined using the obtained testing condition. The relation between the fracture resistance and crack length (*R*-curve) was obtained from this measurement.

2. Calculation

For the calculation of the change in fracture resistance during crack extension, the bending load and crack length during fracture are required. The crack length can be measured as the change of compliance of the specimen. Thus the stress intensity factor at the crack tip and the crack length can be calculated from the load and the deflection of the specimen.

The stress intensity factor on a straight-through notched four-point bend bar specimen is calculated using Equations 1–3 [9, 11]

$$K_I = \frac{P}{BW^{1/2}}\left(\frac{S_1 - S_2}{W}\right)Y \quad (1)$$

$$Y = \frac{3\Gamma_M \alpha^{1/2}}{2(1-\alpha)^{3/2}} \quad (2)$$

0022–2461

$$\Gamma_M = 1.9887 - 1.326\alpha - \frac{(3.49 - 0.68\alpha + 1.35\alpha^2)\alpha(1 - \alpha)}{(1 + \alpha)^2} \quad (3)$$

where K_I is the stress intensity factor and P the testing load. The notations for the shape of the bending bar and the machined notch are shown in Fig. 1.

The changing in compliance of the bending bar caused by crack extension is calculated from Equations 4 and 5

$$C = \frac{1}{E'B}\left(\frac{S_1 - S_2}{W}\right)^2 \int_0^{\alpha} 2Y_{(x)}^2 dx + C_0 \quad (4)$$

$$C_0 = \frac{1}{E'B}\left(\frac{S_1 - S_2}{W}\right)^2 \left(\frac{S_1 + 2S_2}{4W}\right) \quad (5)$$

Because an integral calculation on Equation 4 is required, we obtain an approximated polynomial equation for the calculation of the compliance

$$C = \frac{1}{E'B}\left(\frac{S_1 - S_2}{W}\right)^2 D + C_0 \quad (6)$$

$$D = \frac{\alpha(A_0 + A_1\alpha + A_2\alpha^2 + A_3\alpha^3 + A_4\alpha^4 + A_5\alpha^5)}{(1 - \alpha)^2} \quad (7)$$

Coefficients A_0 to A_5 are shown in Table I.

Equation 3 is for the shape factor at four-point bending. The equation for the shape factor on three-point bending, whose span-to-height ratio is 4, is [12]

$$\Gamma_M = \frac{1.99 - \alpha(1 - \alpha)[2.15 - 3.93\alpha + 2.7\alpha^2]}{(1 + 2\alpha)} \quad (8)$$

This shape factor is also approximated by Equation 7. The coefficients are also shown in Table I.

These equations suggest that the deflection of the bending bar with the notch can be calculated, if the parameters of the specimen, such as stress intensity factor at fracture, Young's modulus, E, notch depth, and the shape of the specimen, are fixed. Fig. 2 shows the relation of the load and deflection of the fracture by applying the parameters of typical silicon nitride (K_{IC} = 5.0 MPa m$^{1/2}$, E = 310 GPa) on four-point bending of 30–10 mm. The height and width of the specimen are 4 and 3 mm, respectively.

For example, this figure shows that if the dimensionless notch depth is 0.2, about 7 μm deflection is required for crack initiation. Once the crack extends, the deflection of the bending bar is fixed with a testing machine, and it does not decrease. Then, the stress intensity factor at the crack front increases with crack extension. It proceeds to catastrophic fracture. On the other hand, if the test is started with a dimensionless notch depth of 0.8, fracture initiates at 6 μm deflection. Once the crack extends, it requires a larger deflection to obtain the same stress intensity factor at the crack front, thus the fracture proceeds stably, even if the sample is brittle, if the machined straight-through notch is deep enough.

Fig. 3 shows the calculated curve for three-point bending. It can be seen that stable fracture can appear at a shallower notch depth on three-point bending, compared to four-point bending. However, in the present work, four-point bending was used, because we did not use the span/height ratio of 4, it being better to avoid the interaction between the upper loading point and the crack front.

3. Experimental procedure

Three kinds of silicon nitride-based ceramics were used for the experiment. Specimen 1 is hot-pressed silicon nitride, supplied by Toshiba Co. Specimen 2 is hot-pressed silicon nitride containing 20 wt % silicon carbide whiskers, supplied by Toshiba Ceramics Co. Specimen 3 is toughened silicon nitride with coarse grains, supplied by NKK Co. Fig. 4 shows scanning electron micrographs of the fracture surfaces of these three ceramics.

R-curve tests were performed with bending bars of 4 mm height and 3 mm width. The load was applied as four-point bending with lower and upper spans of 30 and 10 mm, respectively. The depth of the machined notch was 3.5 mm for the specimen 1, 3.6 mm for the specimen 2, and 3 mm for the specimen 3. The width of the machined notch was 0.1 mm.

In the present work, the testing speed was fixed at a constant crosshead speed of 1 μm min^{-1}. Because crosshead displacement includes the strain of the tes-

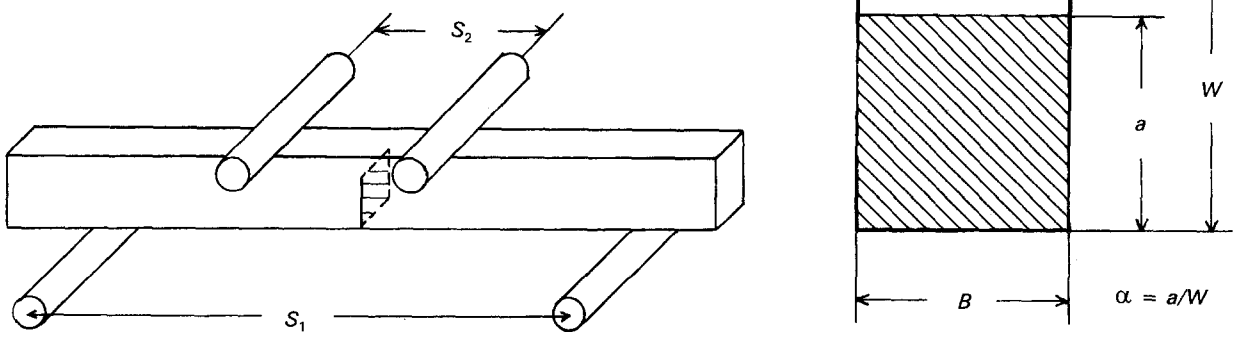

Figure 1 The notations for the bending bar and the straight-through notch.

TABLE I Coefficients for the calculation of the compliance of the bending bar with straight-through notch on four-point or three-point bending by the approximated Equation 7

	Four-point bend	Three-point bend
A_0	0.01362	0.02215
A_1	8.3045	7.9020
A_2	− 21.664	− 23.804
A_3	30.486	38.812
A_4	− 23.668	− 33.028
A_5	7.5197	11.090

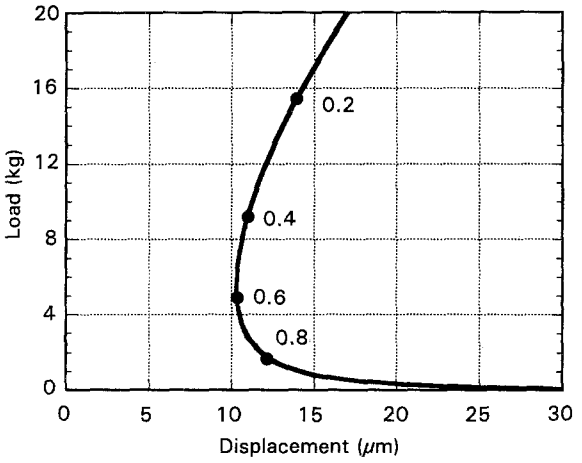

Figure 2 Load–deflection curve obtained from calculation using the parameters of typical silicon nitride for four-point bending. The numbers on the figure are dimensionless notch depth, $\alpha (= a/W)$. If the notch is deeper than 0.56, a larger deflection is required to obtain the same stress intensity factor at the front of the notch.

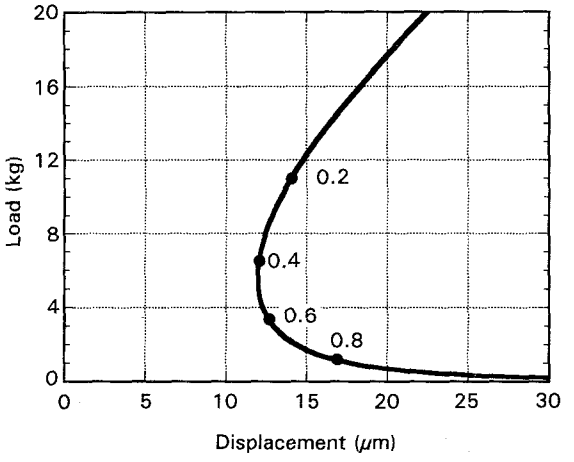

Figure 3 Load–deflection curve obtained from calculation on silicon nitride for three-point bending. If the notch is deeper than 0.46, a larger deflection is required to obtain the same stress intensity factor at the front of the notch. Thus it is easier to obtain stable fracture in three-point bending, than in four-point bending.

ting equipment, the deflection of the specimen is calculated from the Young's modulus of the specimen, and we estimate the strain of the equipment. This is subtracted from the experimental load–displacement curve, and the analysis may then be carried out.

4. Results

Fig. 5 shows the relation between the crosshead displacement and load during the fracture test of specimen 1. As is estimated from the analysis, the load decreases from the onset of fracture, and the decreasing loading rate becomes smaller with crack extension. Therefore, the R-curve obtained from this load–time relation shows a very small increase of fracture resistance, as seen in Fig. 5b. Moreover, in the short crack region, the fracture resistance may be overestimated, because the root radius of the notch is 50 μm. This is not an optimum crack at the beginning of the fracture test.

Fig. 6 shows the load–crosshead displacement relation and R-curve behaviour of specimen 2. In this case, the load–time curve is similar to that of specimen 1. It

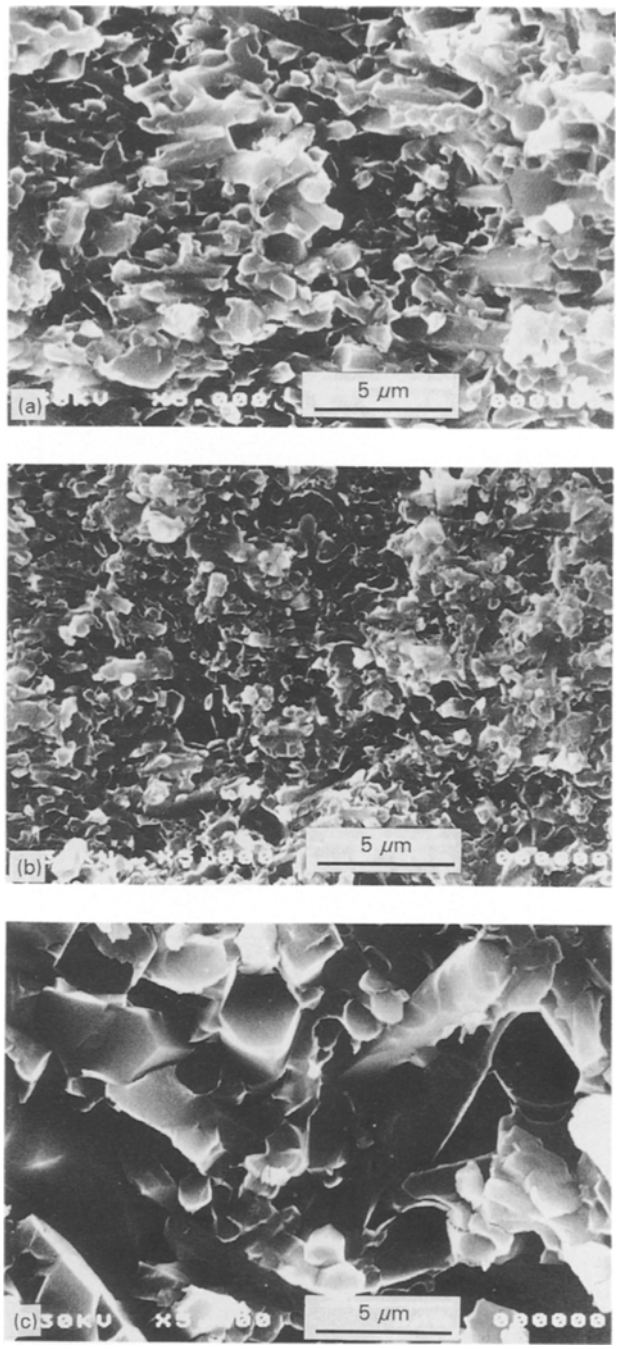

Figure 4 Scanning electron micrographs of the fracture surface of each specimen. (a) Specimen 1 (hot-pressed silicon nitride), (b) specimen 2 (silicon nitride, containing 20 wt % SiC whiskers), (c) specimen 3 (coarse-grained silicon nitride). It should be noted that specimen 2 has the finest microstructure.

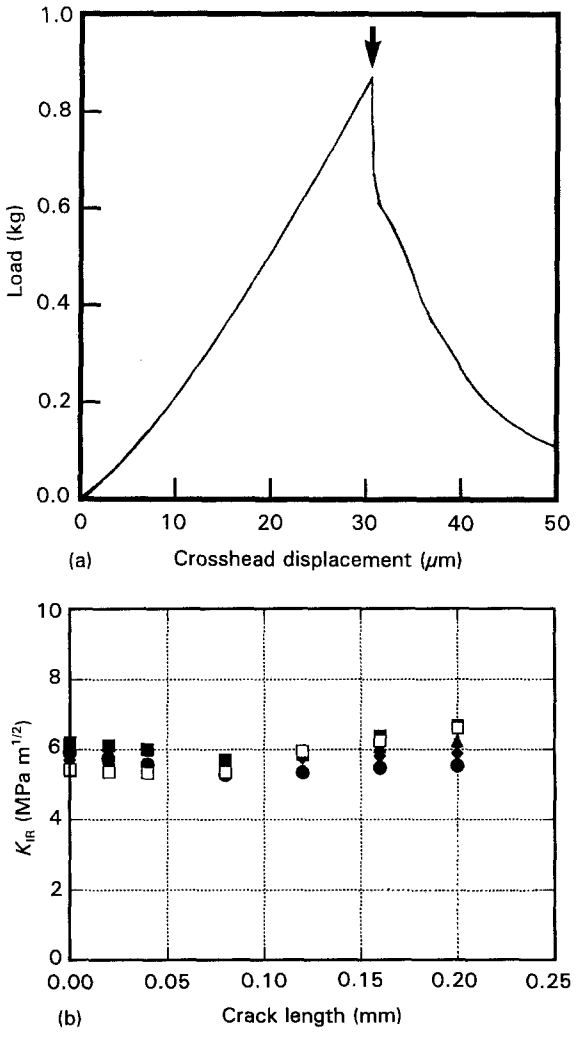

Figure 5 (a) Load–deflection curve and (b) *R*-curve of hot-pressed silicon nitride (specimen 1). The arrow in (a) indicates the starting point of the crack extension. (b) (●) Sample 1, (■) Sample 2, (◆) Sample 3, (▲) Sample 4, (□) Sample 5.

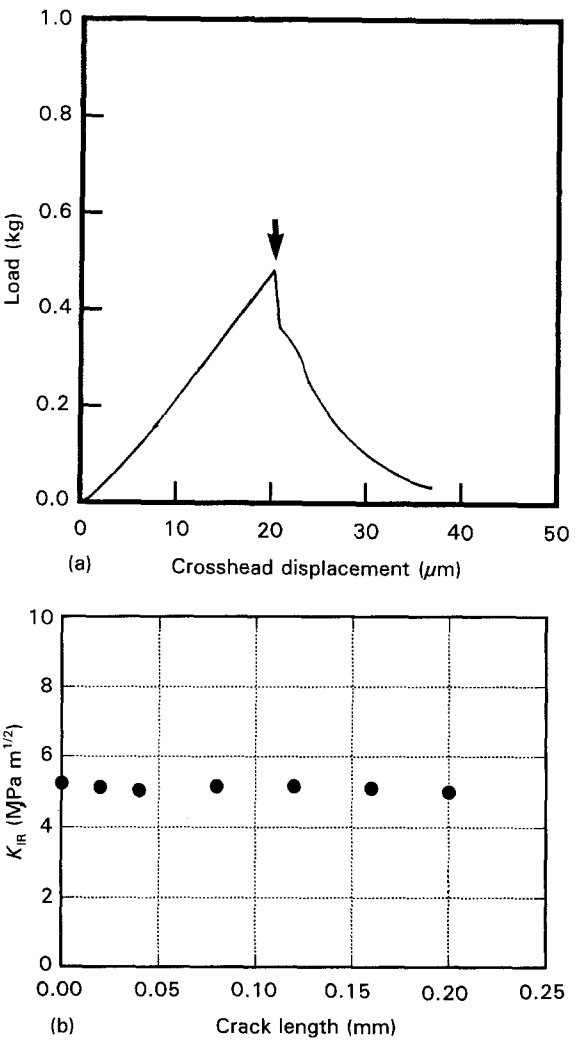

Figure 6 (a) Load–deflection curve and (b) *R*-curve of silicon nitride with silicon carbide whiskers (specimen 2). (b) (●) Sample 1.

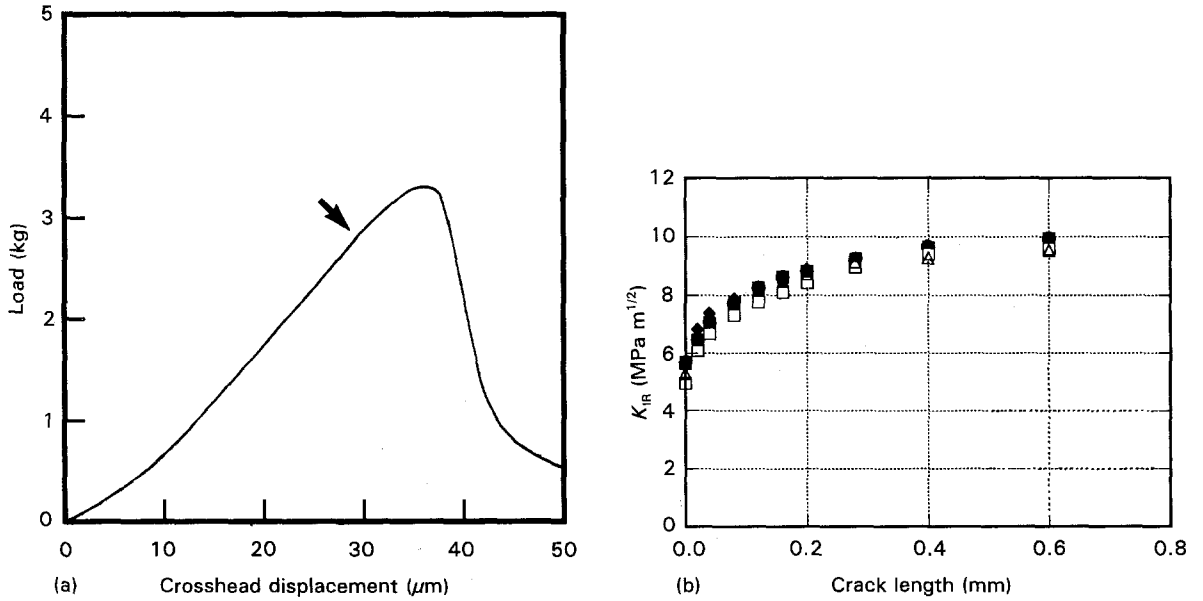

Figure 7 (a) Load–deflection curve and (b) *R*-curve of coarse-grained silicon nitride (specimen 3). (b) (●) Sample 1, (■) Sample 2, (◆) Sample 3, (▲) Sample 4, (□) Sample 5, (△) Sample 6.

shows a steep degradation at the beginning of fracture, and degradation rate of the load becomes smaller with crack extension. Thus an increase of fracture resistance with crack extension is not observed, unlike that obtained for specimen 1.

On the other hand, in specimen 3, the load–time curve does not show a steep decrease of load just after crack initiation, as shown in Fig. 7. Even when fracture starts, the load still increases, and the load–crosshead displacement curve shows a smooth decrease with crack extension after the maximum point. Thus the *R*-curve shows a large increase of fracture resistance, as shown in Fig. 7b. In this case, from the load–time curve, it can be estimated that fracture is very stable. Thus it is relatively easy to obtain the *R*-curve using the single-edge notched beam technique.

5. Discussion

The rise of the *R*-curve is closely related to the microstructure of silicon nitride. As is shown in Fig. 4, specimen 3 has large β-silicon nitride grains and the needle-like shaped grains are combined to each other, thus the fracture surface is very rough. In specimen 1, some needle-like grains are found, but the size of the grains is smaller than those in specimen 3, so that the fracture surface is relatively smooth.

In specimen 2, in spite of containing silicon carbide whiskers, the size of the whisker is not very large (diameter is smaller than 1 μm) compared to the silicon nitride grains, so the silicon carbide whiskers cannot be distinguished from the needle-like β-silicon nitride grains. Moreover, the silicon nitride grains of specimen 2 are smaller than those of specimen 1, because the silicon carbide addition inhibits excess grain growth of silicon nitride. The fracture of specimen 2 is therefore smoother than that of specimen 1. This should be the reason why no rise in the *R*-curve can be observed, and why it is difficult to obtain stable fracture in specimen 2.

6. Conclusions

The R-curve behaviour of three kinds of silicon nitride-based ceramics has been studied by using single-edge notched beam (SENB) specimens. The following conclusions were drawn.

1. The fracture proceeds stably even on brittle ceramic materials, when using a deep-notched SENB specimen. Thus the change in stress intensity factor with the change of crack length can be measured by this technique.

2. For analysis of this technique, integral calculation of the compliance with changing crack length is required. An approximated polynomial equation for this calculation has been obtained.

3. Three kinds of silicon nitride-based ceramics were tested using this technique, which is effective especially for materials which show a large increase of the *R*-curve. Even for a material which shows a small increase in fracture resistance, this technique can be applied.

4. From the fracture surface observation, it is estimated that the increase in the *R*-curve is closely related to the microstructure of the specimen. In particular, it is related to the specimen's grain size.

References

1. K. UENO and S. SODEOKA, *J. Ceram. Soc. Jpn* **100** (1992) 525.
2. S. R. CHOI and J. A. SALEM, *J. Mater. Sci.* **27** (1992) 1491.
3. T. D. FLETCHER, J. J. PETROVIC and J. E. HACK, *ibid.* **26** (1991) 4491.
4. C. OLAGNON, E. BULLOCK and G. FANTOZZI, *J. Eur. Ceram. Soc.* **7** (1991) 265.
5. T. OHJI, Y. GOTO and A. TSUGE, *J. Am. Ceram. Soc.* **74** (1991) 739.
6. J. NAKAYAMA, H. ABE and R. C. BRADT, *ibid.* **64** (1981) 671.
7. N. RAMACHANDRAN and D. K. SHETTY, *ibid.* **74** (1991) 2634.
8. T. FETT and D. MUNZ, *ibid.* **75** (1992) 958.
9. D. MUNZ, R. T. BUBSEY and J. L. SHANNON Jr, *ibid.* **63** (1980) 300.
10. S. SAKAGUCHI, N. MURAYAMA, Y. KODAMA and F. WAKAI, *J. Ceram. Soc. Jpn* **99** (1991) 47.
11. J. E. SRAWLEY and B. GROSS, ASTM Special Technical Publication 601 (American Society for Testing and Materials, Philadelphia, PA, 1976) pp. 559–79.
12. J. E. SRAWLEY, *Int. J. Fract.* **12** (1976) 475.

Received 7 January
and accepted 17 December 1993